ATLANTIS PRESS

Advances in Engineering Research (AER), volume 132
2017 Global Conference on Mechanics and Civil Engineering (GCMCE 2017)

Study of Eccentric Load Coefficient of Pre-stressed Concrete Partial Cable-Stayed Bridge with Corrugated Steel Webs

Yuze Nian[1, a], Junliang Tian[2, b], Suisheng Li[2, c], Wenjuan Liu[2, d], Tao Hu[2, e], Canhua Chang[2, f]

[1]School of Transportation, Southeast University, Nianjing, 210096, China

[2]Highway Administer Department of Zhengzhou, Zhengzhou, 450015, China

[2]Highway Administer Department of Zhengzhou, Zhengzhou, 450015, China

[2]Highway Administer Department of Zhengzhou, Zhengzhou, 450015, China

[2]Highway Administer Department of Zhengzhou, Zhengzhou, 450015, China

[2]Highway Administer Department of Zhengzhou, Zhengzhou, 450015, China

[a]nianyz1990@163.com, [b]13666241@qq.com, [c]1355066319@qq.com, [d]1412268105@qq.com, [e]sjyht2004@163.com, [f]33355938@qq.com

Keywords: corrugated steel webs; partial cable-stayed bridge; finite element computation; eccentric load coefficient

Abstract: In the variable cross-section continuous box girder bridge, due to the complex internal force influence surface of the load, the effect of the box beam geometry on restrained torsional stresses changes along the span of the bridge. Therefore, unified partial load coefficient should not be used over the whole bridge. Through the theoretical analysis and finite element computation based on a real bridge, this paper explores distribution laws of load coefficient along the spans in the variable cross-section pre-stressed concrete partial cable-stayed bridge with corrugated steel webs and proposes practical load coefficient to offer some recommendations for engineering design.

Introduction

CB Company firstly proposed the PC composite beam in 1975. After that, the PC composite beam has a wide development in Japan and other countries [1]. However, until now, there are few researches focused on the effect of eccentric load [2-3]. So, the objective of this paper is to make a systematic research with the finite element analysis. By the load equivalent method, the effect of eccentric load p is divided into the following three variants [4-5] (shown in the dashed box in Figure 1): bending under symmetric load, constrained torsion under torque, distortion under counter force.

The figure 1 shows that, under the eccentric force, the stress at any point on the cross section of the box girder can be divided into three parts: bending stress (symmetric load effect), restrained torsional stress (anti-symmetric load effect), warping and distortion stress (anti-symmetric load effect).

Under the eccentric force, because the empirical estimation method is not applicable to the type of bridge [6-7], the normal stress at a point of the box girder is calculated as the following equation:

$$\sigma_z = \sigma_b + \sigma_t + \sigma_d \tag{1}$$

The shear stress is calculated as the following equation:

$$\tau_z = \tau_b + \tau_t + \tau_d \tag{2}$$

Therefore, the eccentric load coefficient of the normal stress is defined as the following:

$$\xi = \frac{\sigma_b + \sigma_t + \sigma_d}{\sigma_b} \tag{3}$$

The eccentric load coefficient of the normal stress is defined as the following:

$$\eta = \frac{\tau_b + \tau_t + \tau_d}{\tau_b} \quad (4)$$

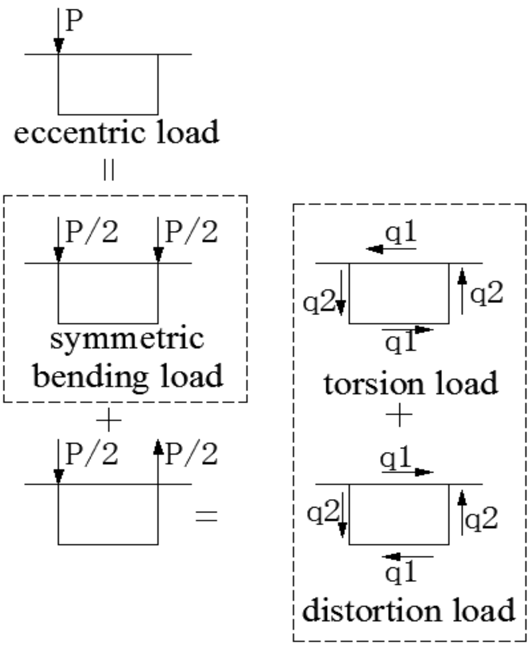

Figure 1 Division of eccentric force P

In these equations, σ_z is normal stress, τ_z is shear stress, ξ is eccentric load coefficient of the normal stress, η is eccentric load coefficient of the normal stress, σ_b is bending normal stress under the symmetrical load, σ_t is restrained torsional normal stress under anti-symmetric load, σ_d is warping and distortion normal stress under anti-symmetric load, τ_b is bending shear stress under the symmetrical load, τ_t is restrained torsional shear stress under anti-symmetric load, τ_d is warping and distortion shear stress under anti-symmetric load.

Project overview

The uniform appearance will assist the reader to read paper of the proceedings. It is therefore suggested to authors to use the example of this file to construct their papers. This particular example uses an American letter format with 25 mm margins left, right, top and bottom.

Chaoyang Bridge is 484.8m long, consisted of 58+118+188+108=472m. The superstructure is partial cable-stayed bridge with corrugated steel webs. P2 and P3 piers use double thin-walled solid Pier and are fixed with the main beam and the main tower. P1 pier uses solid thin-walled Pier and the pot bearing is set on the top of it. Number A4 base is bored pile foundation and the others are all spread foundation. The bridge plane is located in round curve with 3900m radius. The bridge span is designed by the bridge line. Piers are set in radial direction.

The main box beams are made up of C55 concrete, and the main tower is made up of C50 concrete. Base piles of P2, P3 Pier are made up of C30 concrete. The internal tendon is steel strand with high strength and low relaxation. Its standard value of axial tensile strength is 1860MPa, and the steel strand has the diameter for 15.2 mm, area for 139.0, and elasticity modulus for 1.95 MPa. The external tendon is steel strand with epoxy coating, high strength and low relaxation, and the standard value of axial tensile strength is 1860MPa. The thickness of corrugated steel is 12~ 24mm, and the type is 1600. General arrangement of the bridge is shown in Figure 2.

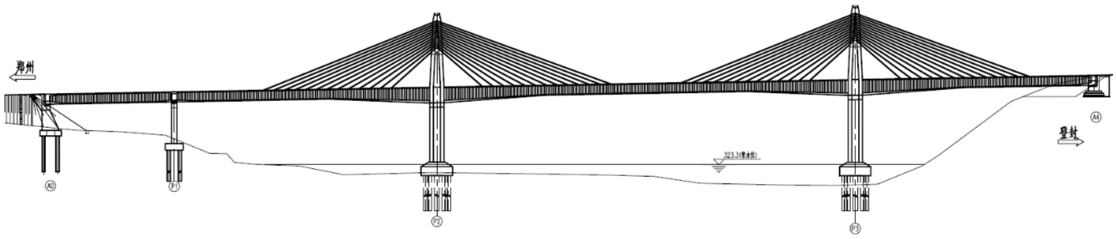

Figure 2 General arrangement

Structure analysis

This article adopts the finite element software ANSYS15.0 to build the whole bridge model to carry on the numerical simulation, as shown in Figure 3. The concrete and concrete diaphragm plate is simulated by Solid45 entity unit, corrugated steel web is simulated by the Shell 181 units, cables and pre-stressed steel (including in vivo and in vitro) is simulated by Link8 bar units, and the main joist steel beam is simulated by Beam44 element. The amount of bridge units is 1167684.

Refer to the purpose of static load test of this bridge and assess regulations of the highway bridge bearing capacity (JTG/T J21-2011), the efficiency coefficient of static test load η_q has the range:

$$0.95 \leq \eta_q \leq 1.05 \tag{5}$$

$$\eta_q = \frac{S_s}{S' \cdot (1+\mu)} \tag{6}$$

In the equations, S_s is the maximum value of internal force of control sections under the static test load. S' is the value of the most adverse effect of testing load, and for this bridge, the value is calculated under the bridge design load. μ is the impact coefficient. η_q is the efficiency coefficient of static test load.

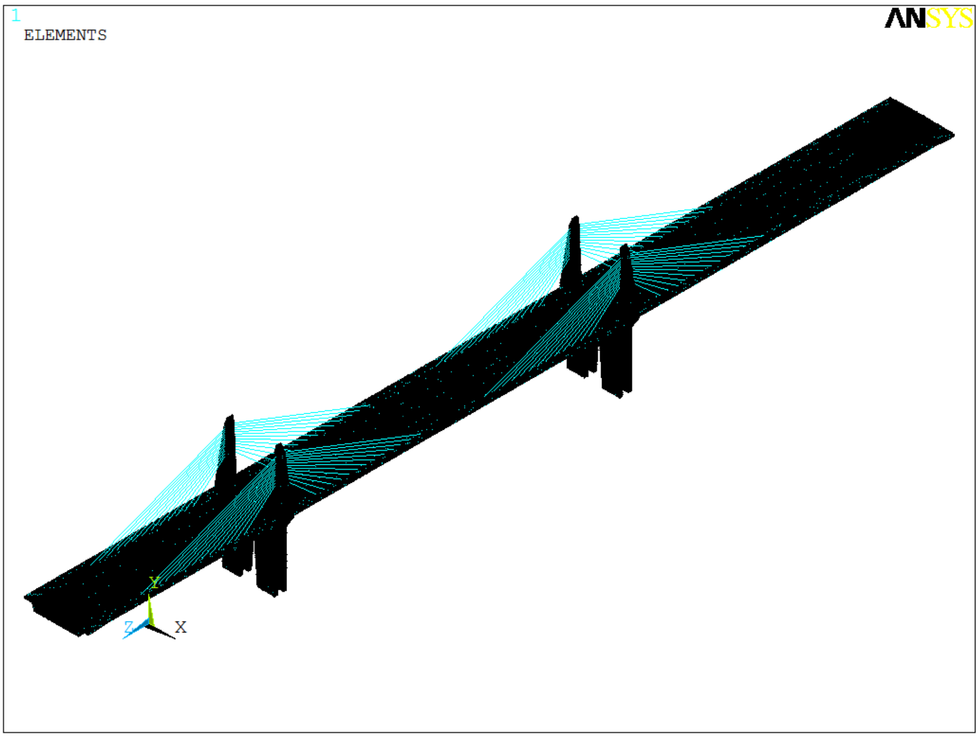

Figure 3 Whole bridge model

Test load is determined by bending moment of control section under serviceability limit state loads. Use the maximum value of design live load as the control value of test load. Impact factor is calculated by the standard. Fundamental frequency is calculated by the FEM. The influence lines of internal force of cross sections are shown in Figure 4, in which (a), (b), (c), (d) is namely the internal force influence lines of 58m, 118m, 188m and 108m cross sections.

As shown in Figure 5, along the longitudinal direction, there are 15 main control sections Z1 - Z15. And the arrangement of monitoring stations on each key section is shown in Figure 6. Each section has 10 monitoring stations of eccentric load coefficient of normal stress D1 ~ D10, and 3 monitoring stations of eccentric load coefficient of shear stress D11, D12, D13. This paper takes two loading conditions to study eccentric load coefficient of partial cable-stayed bridge with corrugated steel webs, as shown in Figure 7, loading symmetrical P / 2 (two) and eccentric load at

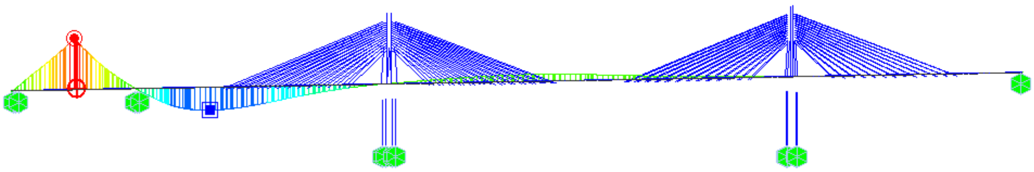

(a)

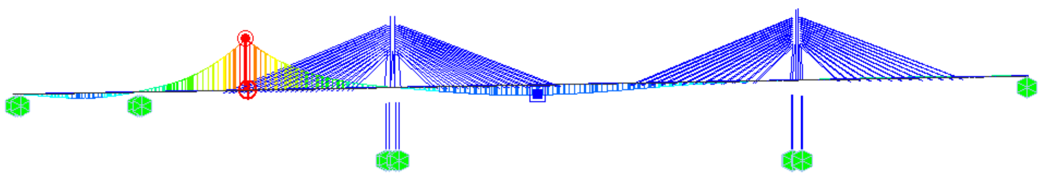

(b)

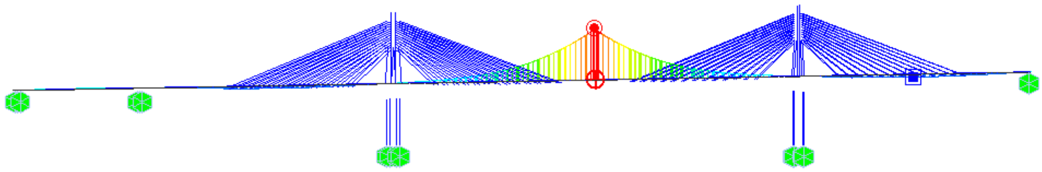

(c)

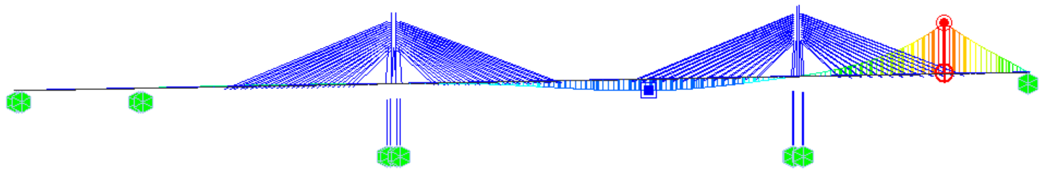

(d)

Figure 4 Internal force influence lines of cross sections

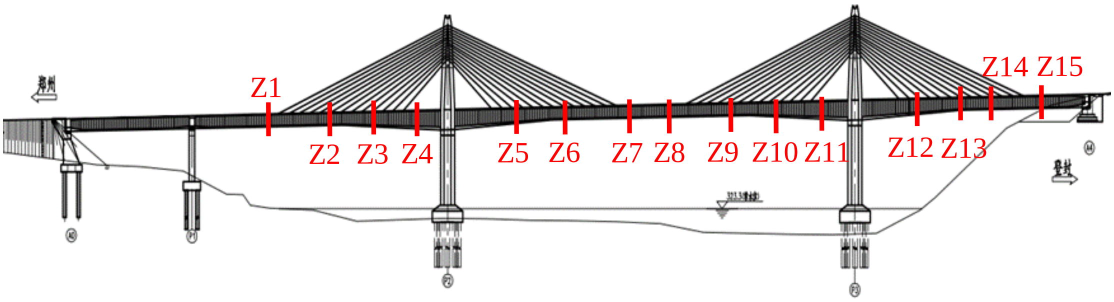

Figure 5 Location of main control sections Z1~Z15

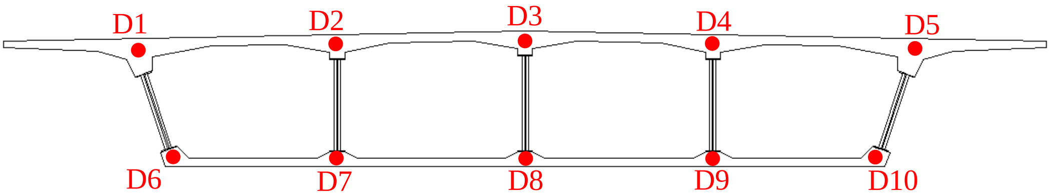

Figure 6 Monitoring stations on the control section

the across. P is 800kN, the summation of the weight of 20 40-ton double-axle trucks. The load position along the longitudinal direction is 118m the second across the span, 188m the third across, and the forth across.

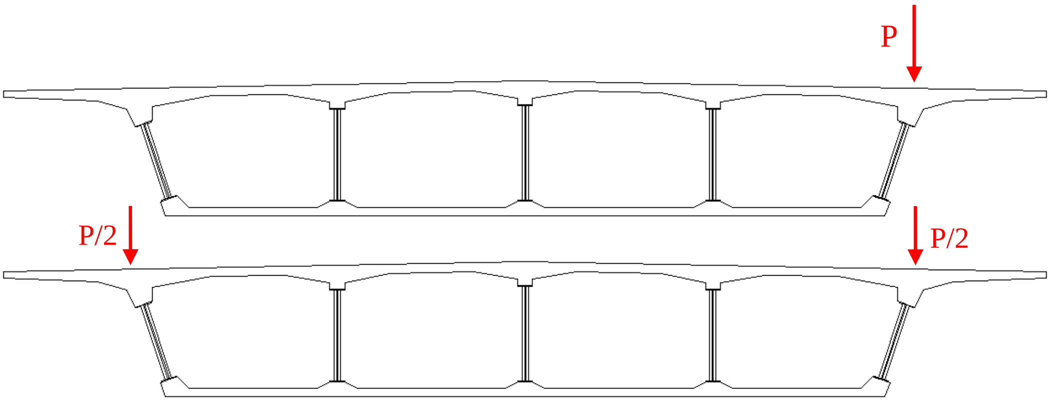

Figure 7 symmetrical and eccentric load

Calculations of 188m the third across section Z8 (Figure 7) are listed in Table 1. From the table, the eccentric load coefficient of normal stress of section Z8 is 1.38, and the maximum value of monitoring points appears in D10, namely the intersect angle point between the abdominal board on the eccentric load side and floor. The calculation results are reasonable and consistent with related researches. The eccentric load coefficient of shear stress of section Z8 is 1.68, larger than the empirical eccentric load coefficient of shear stress under live load. It means that the corrugated steel webs have great effect on the empirical eccentric load coefficient of shear stress. The maximum value of monitoring points appears in D13, namely the midpoint of the abdominal board on the eccentric load side. The calculation results are reasonable and consistent with related researches. Compared with the section Z5, Z6, Z7, section Z8 is closer to the cross, and the effect of eccentric load on the cable-stayed bridge with low pylon is heavier. Therefore, it is necessary to appropriately enlarge cross-loaded coefficients in design to enhance the stability of the bridge.

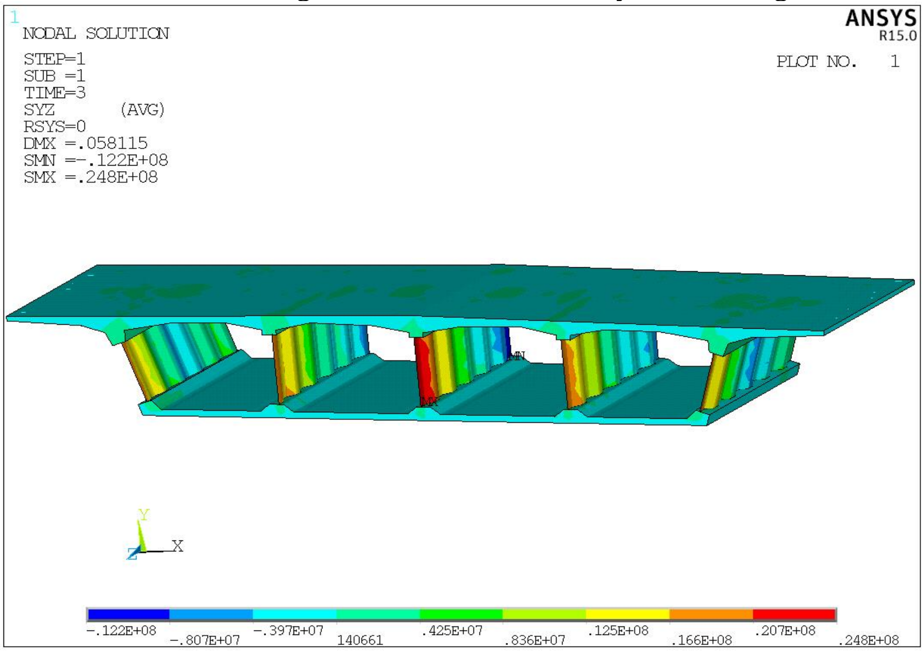

Figure 8 Shear stress in section Z8

Table 1 Normal stress and shear stress in section Z8

Monitoring point	Section Z8			
	Normal stress/Pa			
	Bridge load	Symmetrical load	Eccentric load	Eccentric load coefficient
D1	-7131910.63	-7228572.66	-7194892.8	0.651570943
D2	-8414116.84	-8501797.79	-8489797.9	0.863141424
D3	-8691659.34	-8773720.03	-8786114.01	1.151034314
D4	-7824882.79	-7907696.89	-7931652.17	1.289265717
D5	-6113452.52	-6212316.51	-6269212.92	1.575501859
D6	-15338789.2	-15103654.7	-15253892.8	0.361054631
D7	-15177198.2	-15023990.2	-15065590.7	0.728470445
D8	-15109877.1	-14980417.1	-14963596.1	1.129932025
D9	-14863775.1	-14710569.1	-14669265.76	1.269593474
D10	-14599135.5	-14380484.8	-14295942.32	1.386655417

Analysis results of all test sections Z1~Z15, and get the distribution of eccentric load coefficient of normal stress of the cable-stayed bridge with low pylon along the longitudinal direction (Table 2 and Figure 9). Figure 9 shows that the normal stress changes along the span of

Table 2 Distribution of eccentric load coefficient of normal stress and shear stress of the cable-stayed bridge with low pylon along the longitudinal direction

Section	Eccentric load coefficient	
	Normal stress	Shear Stress
Z1	1.18	1.68
Z2	1.09	1.59
Z3	1.25	1.73
Z4	1.29	1.69
P2 Pier	-	-
Z5	1.25	1.54
Z6	1.32	1.42
Z7	1.35	1.49
Z8	1.38	1.68
Z9	1.34	1.63
Z10	1.33	1.64
Z11	1.25	1.59
P3 Pier	-	-
Z12	1.18	1.57
Z13	1.13	1.55
Z14	1.27	1.68
Z15	1.24	1.52

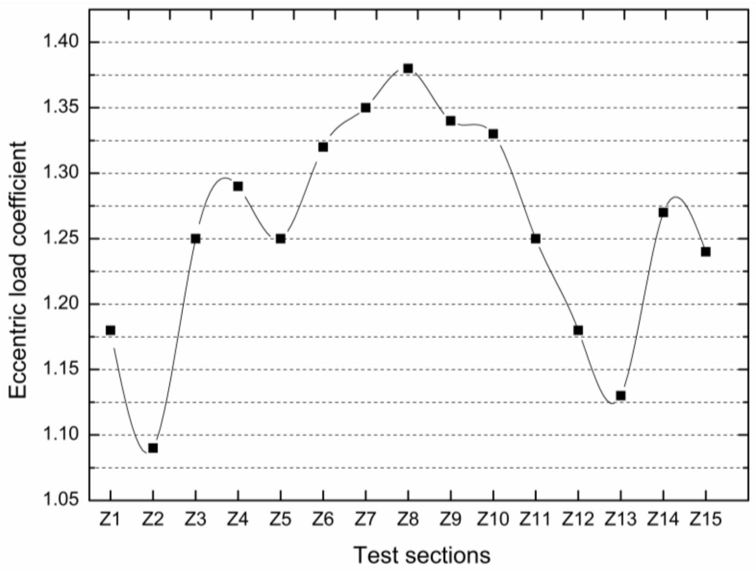

Figure 9 Distribution of eccentric load coefficient of normal stress and shear stress along the longitudinal direction

the bridge, the effect of eccentric load on normal stress is more obvious. The average of eccentric load coefficient of normal stress is 1.25.

Conclusion

(1) Eccentric load coefficient of normal stress and shear stress of the cable-stayed bridge with low pylon with corrugated steel webs is not a constant along the longitudinal direction. Different sections have different coefficients, the largest in the across and decreasing on both sides.
(2) Eccentric load coefficient of normal stress and shear stress of the cable-stayed bridge with low pylon with corrugated steel webs changes obviously in the mutation between the uniform section and non-uniform section, characterized by that the eccentric effect is significant in the location of the high beam.
(3) The calculation results are reasonable and consistent with related researches. The normal stress changes along the span of the bridge, and the effect of eccentric load on normal stress is more obvious. It is necessary to appropriately enlarge cross-loaded coefficients in design to enhance the stability of the bridge. The distribution of eccentric load coefficient from the analysis can be used in some situation and can be a reference for the design and analysis of continuous girder bridge with variable cross-section.

References

[1] Liu Haiyan. List of PC box-girder with corrugated steel webs built in Japan [J].2002,30(1):58 ～ 59.
[2] Li Hongjiang. Experimental Study and Analysis on Torsion and Distortion of Box-girder with Corrugated Steel Webs [D]. Southeast University.2003.
[3] Ma Lei. Study on Bending and Torsion of Single Box Multi-cell Girder with Corrugated Steel Webs [D]. Southeast University.2015.
[4] Guo Jinqiong. Box Beam Design Theory [M]. Beijing. China Communications Press. 1991.
[5] Liu Zhao. Theory of Conceptual Design and Analysis of Bridges [M]. Beijing. China Communications Press. 2010.
[6] Guo Yi, Ye Jianshu, Wan Hongyan. Study on Load Test of Pre-stressed Concrete Box Girder [J]. Journal of Heilongjiang Institute of Technology, 2002(04):14-16.
[7] C. C. Fu，Yao T Hsu. Bridge Diaphragm Elements with Partial Warping Restraint[J]. Journal of structural engineering，1994120(11).